



HAL
open science

Molecular simulation of realistic membrane models of alkylated PEEK membranes

Elena Tocci, Pluton Pullumbi

► **To cite this version:**

Elena Tocci, Pluton Pullumbi. Molecular simulation of realistic membrane models of alkylated PEEK membranes. *Molecular Simulation*, 2006, 32 (02), pp.145-154. 10.1080/08927020600654645. hal-00516539

HAL Id: hal-00516539

<https://hal.science/hal-00516539>

Submitted on 10 Sep 2010

HAL is a multi-disciplinary open access archive for the deposit and dissemination of scientific research documents, whether they are published or not. The documents may come from teaching and research institutions in France or abroad, or from public or private research centers.

L'archive ouverte pluridisciplinaire **HAL**, est destinée au dépôt et à la diffusion de documents scientifiques de niveau recherche, publiés ou non, émanant des établissements d'enseignement et de recherche français ou étrangers, des laboratoires publics ou privés.

**Molecular simulation of realistic membrane models of
alkylated PEEK membranes**

Journal:	<i>Molecular Simulation/Journal of Experimental Nanoscience</i>
Manuscript ID:	GMOS-2005-0070.R2
Journal:	Molecular Simulation
Date Submitted by the Author:	23-Feb-2006
Complete List of Authors:	Tocci, Elena; ITM-CNR, Research Institute for Membrane Technology Pullumbi, Pluton; Air Liquide, Research Center
Keywords:	Glassy polymer membrane, molecular simulation, diffusivity and solubility, permeability, small gas molecules

SCHOLARONE™
Manuscripts

1
2
3
4
5 **Molecular simulation of realistic membrane models of alkylated PEEK**
6 **membranes**
7

8
9
10 E.TOCCI¹ and P. PULLUMBI*²
11

12
13 ¹Research Institute for Membrane Technology ITM-CNR, Via P. Bucci, Cubo 17/C, c/o
14 Università della Calabria I-87030 Rende (CS), Italy
15

16
17
18 ²Air Liquide, Centre de Recherche Claude-Delorme, B. P. 126, Les-Loges-en-Josas,
19 78354, Jouy-en-Josas Cedex, France
20
21

22
23 **Abstract**
24

25 Atomistic molecular modelling has proven to be a useful tool for the investigation of
26 transport properties of small gas molecules in polymer membrane matrices. The quality
27 of the predictions of these properties based on molecular simulation depends principally
28 on the quality of the membrane model. The predicted gas transport properties of small
29 gas molecules in the same glassy polymer membrane show often a large scatter in gas
30 diffusion and solubility simulated values. In order to reduce the scatter in predicted gas
31 transport properties in glassy polymer membranes, numerical analysis of structural
32 features of the membrane model is used for pre-selecting only the realistic ones for
33 further simulations using transition state theory (TST) approach. Simulation results of
34 gas solubility and diffusion in alkylated poly-ether-ether-ketone (PEEK) membranes
35 will illustrate the approach.
36
37
38
39
40
41
42
43
44
45
46
47
48
49
50

51
52
53
54
55
56
57
58
59
60
Keywords: Glassy polymer membrane, molecular simulation, solubility, diffusion,
permeability, small gas molecules.

1. Introduction

Transport properties of small molecules in amorphous polymer matrices play an important role in many industrial applications such as gas separation of mixtures, packaging applications ranging from food conservation to controlled drug & cosmetics release, to special coatings for protecting specific substrates from gases. The prediction of transport properties of small molecules through polymer matrices would allow for the rational selection of polymer materials used in these applications and their future optimal design. Although there has been reported an increasing number of studies on this subject over the last decades[1-20], the prediction of transport properties of gas molecules through glassy polymer membranes remains a difficult target. In many of the recent studies reporting molecular simulation prediction of diffusion and solubility of small gas molecules in several membrane models of the same glassy polymer a great scatter of the predicted values is observed. These results clearly indicate that the quality of the packing of the polymer chain into an amorphous cell membrane model strongly impacts the predicted gas transport properties.

The potential application of a polymer as a separation membrane depends upon the possible throughput and the purity of product[21-23]. This means that both the permeability of the gas that is transported more rapidly and the selectivity should be as large as possible. The permeability coefficient P of a small molecule through a polymer membrane is defined as the product of the diffusion coefficient D (kinetic parameter) and of the solubility coefficient S (thermodynamic parameter). The estimation of these coefficients can be done, either by Molecular Dynamics (MD) and Grand Canonical Monte Carlo (GCMC) simulations, or by applying the TST method provided that the quality of the membrane amorphous cells used in the calculation represent the real distribution of torsion angles, of the free volume and its distribution, as well as the structural, conformational and volumetric properties of polymer membranes. The selectivity of a polymer membrane for a pair (i,j) of gas molecules is characterized by the ideal separation factor α_{ij} defined in (1) :

$$\alpha_{ij} = \frac{P_i}{P_j} = \frac{S_i D_i}{S_j D_j} \quad (1)$$

1
2
3
4
5
6
7
8
9
10
11
12
13
14
15
16
17
18
19
20
21
22
23
24
25
26
27
28
29
30
31
32
33
34
35
36
37
38
39
40
41
42
43
44
45
46
47
48
49
50
51
52
53
54
55
56
57
58
59
60

Following this definition the selectivity of a membrane is the product of solubility selectivity (S_i/S_j) and diffusion selectivity (D_i/D_j). In the case of glassy polymer membranes the overall selectivity is mainly controlled by diffusion selectivity.

In the past twenty years, the control of gas permeability and permselectivity of polymer membranes has become a subject of strong research with worldwide participation in both industrial and academic laboratories[22, 24-27]. To achieve such control, it has been necessary to reach a good understanding of the relationship between the properties of the polymers and their gas transport properties. However, it has been found that simple structural modifications, which lead to increase in polymer permeability usually, cause loss in permselectivity and vice versa. This so-called "trade-off" relationship has been well described in the literature[21, 24, 25, 28, 29]. The upper bound limit is not fixed in the α -P space but moves with time as new polymers with optimised structures become available.

Recent studies indicate that in addition to the free volume content, gas transport parameters depend upon the backbone chain rigidity, its segmental mobility, the inter-chain distance and the chain interactions. For example the introduction of bulky alkyl substituents opens up the polymer matrix resulting in a greater permeability. Also the reported introduction of n-alkyl side groups on a polymer backbone increases the side-chain flexibility as well as the membrane free volume with an overall increase of the permeability[21, 22, 30-32].

Modified polyether-ether-ketone (PEEK-WC)[33, 34] are of considerable interest due to their excellent mechanical toughness, thermo-oxidative stability, solvent resistance and high transition temperature. In addition PEEK-WC, in contrast to the traditional crystalline PEEK, is soluble in a wide range of solvents and can be cast into flexible tough films[35-38]. In the last decade considerable effort has been spent to introduce chemical modifications in this class of polymers in order to obtain better physical properties and to build-up membranes for electro dialysis, gas dehumidification and gas separation. Relatively few atomistic simulations have been performed on this class of

1
2
3
4
5 polymers[14, 39, 40], since generating an appropriate equilibrium conformation is more
6 computationally challenging than with an atactic polyolefins[41].
7
8
9

10 The purpose of the molecular simulations performed in this study is to demonstrate the
11 importance of realistic representation of structural features of glassy polymer
12 membranes models for predicting gas transport properties using the MD technique. A
13 methodology for generating realistic models of membranes will be used for finding a
14 relationship between chemical structure and conformational properties of alkylated
15 PEEKs and gas permeabilities through them. Details of simulated self-diffusion,
16 solubility and structural properties will be reported for the unsubstituted PEEK and for
17 three synthesized alkylated PEEKs[42], namely dimethyl PEEK-WC (DMPEEK),
18 tetramethyl PEEK-WC (TMPEEK) and di isopropyl dimethyl PEEK WC
19 (DIDMPEEK). The monomer structure, experimental density and the glass transition
20 temperature of the four poly(ether ether ketone)s is reported in Figure1.
21
22
23
24
25
26
27
28
29
30
31
32
33
34
35
36
37
38
39
40
41
42
43
44
45
46
47
48
49
50
51
52
53
54
55
56
57
58
59
60

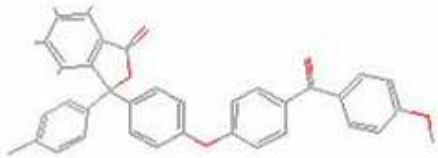

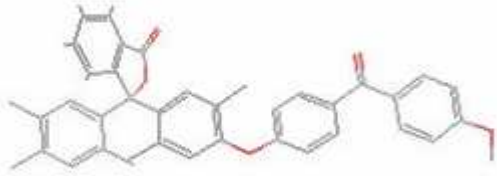
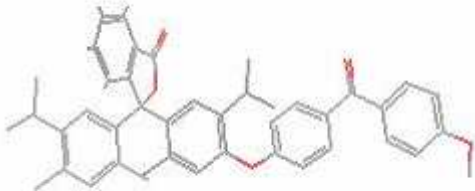
Monomer Structure	ρ (g cm ⁻³)	T _g (K)
 <p>PEEK-WC</p>	1.25	501
 <p>DMPEEK</p>	1.247	512
 <p>TMPEEK</p>	1.195	519
 <p>DIDMPEEK</p>	1.140	514

Figure 1: Monomer structures and experimental data of selected PEEKs

2. Computational Method

The estimation of the diffusion coefficient D , of the solubility coefficient S (and consequently of permeability P) of small permeant molecules in a polymeric membrane is strongly dependent on the quality of the amorphous cell used in the calculation. This is particularly true in the case of stiff chain polymers containing aromatic moieties. In this study several amorphous packing of the polymer chain for the four PEEKs, reported in Figure 1, followed by model equilibration and prediction of gas transport properties, have been carried out using the InsightII (400P+) molecular modelling package[43] for materials sciences together with COMPASS (Condensed-phase Optimized Molecular Potentials for atomistic Simulation Studies) force field[44, 45] on two SGI Octane machines.

For each of the poly(ether-ether-ketone) polymer three independent atomistic bulk models were generated. The cubic basic volume element first has been filled with segments of a growing chain under periodic boundary conditions following a combination of the Theodorou-Suter[41] chain-generation approach and the Meirovitch's scanning method[46] reproducing the natural distribution of conformation angles. In the case of polymers without aromatic moieties the size of the volume element can be chosen so as to reproduce the experimentally observed or theoretically predicted macroscopic density of the relevant polymer. For partly aromatic polymers, however, the chain packing stage has to be performed at very low densities to avoid ring-catenation. We have inserted "solvent" molecules in the initial phase of amorphous cell construction in order to avoid ring ring-catenation. Different multistage equilibration procedures after sequential removal of "solvent" molecules followed by energy minimisation and MD simulations have been tested in order to be able to reproduce realistic models of the polymer membranes. We have used the variation of Surface to Accessible Volume ratio as well as its gradient, with the probe radius used to calculate the accessible volume and surface of each amorphous cell, as a descriptor of the "goodness" of each packing at an intermediary stage of construction. After the elimination of the non-realistic boxes we have finally generated 3 realistic amorphous cells for each of the polymers. During the final amorphous cell generation the conformation and non-bonded pair interaction terms in the force field (torsion, non-bonded and coulomb interactions) have been first appropriately scaled down by 1:1000

1
2
3
4
5 followed by 1000 steps of conjugate gradient minimization and 1ps of NPT dynamics
6 and then the interactions were scaled up to original values in 6 steps (torsions in three
7 steps 1:100, 1:10 and 1:1 with intermediary minimisation and NPT 1ps relaxation
8 followed by “non-bonded and coulomb” in three steps 1:100, 1:10 and 1:1 with
9 intermediary minimisation and NPT 1ps). Finally a series of seven MD 5ps compression
10 runs [(NPT,1GPa, 300K) (NVT, 600K) (NVT, 300K) (NPT, 0.1GPa, 300K) (NPT,
11 0.01GPa, 300K) (NPT, 0.001GPa, 300K) (NPT, 0.0001GPa, 300K, 30ps)] followed by
12 300ps NVT (300K) have been performed for each amorphous cell to match the
13 experimental density.
14
15
16
17
18
19
20
21

22 The permeation of small molecules through dense polymeric membranes occurs by the
23 solution-diffusion mechanism involving two key steps[45, 47-49]. In the first step, the
24 penetrant molecules are dissolved and sorbed in the polymer matrix, while in the second
25 one they diffuse through the medium. MD simulations are useful for calculating
26 diffusion coefficients in rubbery polymers but do not sample large enough time scales to
27 provide reliable information about glassy diffusion. The difficulties lie in the extremely
28 broad distribution of gas molecule jump rates. It is known that the diffusion of a
29 penetrant in a glassy polymer involves occasional jumps between cavities through the
30 opening of a channel[12, 15, 50]. Jumps are rare events and the time between them is
31 much shorter than the times governing matrix relaxation processes. For these reasons
32 the diffusion coefficient can be estimated using Transition-State theory (TST).
33
34
35
36
37
38
39
40

41 TST provides an approximate way to calculate the rate coefficient, k_{jump} , of each
42 possible jump from cavity to cavity in a polymer microstructure. Gusev and Suter
43 implemented the original TST method giving the polymer some flexibility[51, 52]
44 assuming that the polymer atoms, in a sorption site, execute uncorrelated harmonic
45 vibrations around their equilibrium positions to accommodate the guest molecules. The
46 behaviour and properties of the small gas molecules can be described[53, 54] with a
47 time independent single-particle distribution function $\rho(\mathbf{r})$, where \mathbf{r} is the position. The
48 thermal fluctuations of the position of all atoms Δ are described by an isotropic
49 Gaussian functional form. The smearing factor $\langle \Delta^2 \rangle$ is a parameter in the homogeneous
50 isotropic approximation, which can be evaluated from atomistic trajectories of the
51 polymeric matrix by means of short-scale MD simulations of the host matrix without
52 dissolved molecules. The averaging time at which the smearing factor $\langle \Delta^2 \rangle$ is
53
54
55
56
57
58
59
60

1
2
3
4
5 determined, should be the most frequent residence time τ of a probe molecule in the
6 void. Since the value of the average time of penetrant molecules depends on the thermal
7 vibrations of the polymer matrix an iterative procedure is used, starting with setting,
8 rather arbitrarily, $\langle \Delta^2 \rangle = 0.3-0.4 \text{ \AA}$ and computing $\rho(\log\tau, \langle \Delta^2 \rangle)$.
9
10
11
12
13
14

15 **2.1 Preparation of amorphous cell packings**

16
17
18 The Simulations of the amorphous cells of the membrane have been carried out using
19 the InsightII (400P+) molecular modelling package of Accelrys and the COMPASS
20 force field[44, 53-55] going through the following steps :

21
22
23
24
25 1. Single repeat units of each of the four polymers have been constructed using the
26 polymer BUILDER module of Insight II (400P+) molecular modelling package[43].
27 Charge groups have been assigned to fragments of each repeat unit and used for their
28 energy minimisation employing a standard algorithm starting with a steepest-descent
29 stage, switching to conjugate gradient when the energy derivative reaches 1000
30 kcal·mol⁻¹Å⁻¹ followed by a Newton-Raphson optimisation algorithm. The final
31 convergence criterion was to meet a derivative of less than 0.001 kcal·mol⁻¹Å⁻¹.
32
33
34
35
36
37

38
39 2. The isolated initial chain configurations of unsubstituted and alkylated PEEKs
40 with a degree of polymerization of 100 have been constructed using the
41 POLYMERISER module of Insight II (400P+) molecular modelling package. The
42 backbone dihedral angle was set to random and the individual PEEK polymer chains
43 were rapidly optimised (500 steps) using a group-based cut-off of 12 Å^o with a spline-
44 width of 1.0 Å^o and a buffer-width of 0.5Å^o using a three stage minimization
45 algorithm: steepest descents for initial relaxation (energy derivative less then 1000
46 kcal·mol⁻¹Å⁻¹) conjugate gradients (energy derivative less then 10 kcal·mol⁻¹Å⁻¹) and
47 Newton-Raphson (energy derivative of less than 0.001 kcal·mol⁻¹Å⁻¹). Each optimised
48 chain was briefly relaxed through a 300 ps long molecular dynamics run with constant
49 temperature (300K^o) and time step of 1 fs. The Andersen method[56] was used to
50 control the temperature. The relaxed chains were submitted again to optimisation
51 following the three stage protocol described above.
52
53
54
55
56
57
58
59
60

1
2
3
4
5 3. Bulk amorphous polymer structures have been generated using Amorphous
6 Cell, which involves construction of chains in a periodic cell, at 303 K, with a RIS-
7 based bond-by-bond construction method and taking account of bond torsion
8 probabilities and bulk packing requirements[41, 53]. To reduce the influence of chain
9 ends on the simulations only a single long chain has been utilised. Several spacer
10 molecules have been introduced in the amorphous cell to avoid the artefacts of
11 catenated phenylene rings or a sparring of side groups or backbone chains through ring
12 sub-structures as well as to confer realistic conformation to packed polymer chain. The
13 spacers representing small obstacles (200 methanol molecules and 3 sets of 200 argon
14 atoms) have been added sequentially in the simulation box before packing of the
15 polymer. After a first relaxation using the Basic-Refine protocol of InsightII (400P+)
16 employing an initial energy minimization followed by a NVT MD relaxation at 300K
17 and final energy minimisation the spacer molecules have been removed in the reverse
18 order of their introduction in the box (first the 200 methanol molecules and than 3 sets
19 of 200 argon atoms) followed by energy minimisation and MD relaxation-compression
20 cycles after removal of each set.
21
22
23
24
25
26
27
28
29
30
31
32

33
34 4. The spacer-free packing models, with a reduced density in comparison to the
35 experimental value, have been subjected to extensive equilibration procedures
36 composed of sequences of energy minimization and NPT and NVT-MD and annealing
37 simulations combined with force field parameter (torsion, non-bonded and coulomb
38 interactions) scaling steps reported in Table1 associated with intermediary NVT and
39 NPT MD relaxations as discussed above. The final equilibration stage is carried using a
40 NVT run at 300K for 300ps duration time.
41
42
43
44
45
46
47
48
49
50

51 5. The goodness of each model has been analysed, before the complete
52 equilibration procedure has been performed at an intermediate stage when the density of
53 the packing boxes was at a value corresponding at the 90% of the experimental value.
54 The variation of surface-to-volume ratio as well as its gradient with the probe radius has
55 been used to analyse the accessible volume of each cell. The “Free Volume” routine
56 implemented in Cerius2 simulation software[43] was used to calculate the accessible
57 volumes and surface areas using a probe sphere (with an adjustable radius) that is rolled
58 through the amorphous periodic structure to generate a solvent accessible, internal void
59
60

1
2
3
4
5 volume that has a corresponding internal surface area. Due to the size variation of probe
6
7 molecules, the probe can only 'see' a subset of the total free volume which is termed
8
9 accessible volume. The calculation method is very similar to Connolly surface
10
11 calculations and employs a grid method.

12
13
14 6. After this stage, by using with several cycles of NPT-MD (constant particle
15
16 number, temperature and pressure) runs at pressures of thousands of bars the density of
17
18 the systems has been increased. Besides, simulated annealing runs with temperatures up
19
20 to 1000 K and NVT dynamics at 303 K were used to further relax the polymer structure.
21
22 The general simulation condition used were: minimum image boundary condition to
23
24 make the system numerically tractable and to avoid symmetry effects; a cutoff distance
25
26 of 15 Å with a switching function in the interval 13.5–15 Å. Through the dynamics, the
27
28 Andersen[56] temperature control and the Berendsen[57] pressure control method have
29
30 been used. The side length of the bulk models is of about 3 nm for all PEEKs.

Stage of equilibration	Scaling factor for the conformation energy terms in the forcefield	Type of non-bonded interaction energy terms (E_{vdW})	Type of non-bonded interaction energy terms ($E_{Coulomb}$)
1	0.001	0.001	0.001
2	0.01	0.001	0.001
3	0.1	0.001	0.001
4	1	0.001	0.001
5	1	0.01	0.01
6	1	0.1	0.1
7	1	1	1

31
32
33
34
35
36
37
38
39
40
41
42
43
44
45
46
47
48
49
50
51
52
53
54 Table1: Scaling procedure of FF energy terms torsion, non-bonded and coulomb interactions.
55
56
57
58
59
60

2.2 Calculation of gas transport data in alkylated PEEK membranes

The transition state theory (TST) after Gusev and Suter [41], as implemented in InsightII (400P+)[43], has been used to study the thermodynamics and transport of the small gas molecules, oxygen, nitrogen and carbon dioxide, respectively, in selected PEEKs packings. Diffusion coefficients (D) and gas solubility (S) in the matrix have been estimated, and the permeability coefficients (P) have been calculated by direct product of D and S. The calculation has been carried out in two steps. In the first step, the solubility (S) of the respective gas is evaluated. A 3D orthogonal lattice grid with a constant spacing of 0.3 \AA has been used to estimate solute distribution function in the matrix by calculating the Helmholtz free energy between the gas molecule inserted at each grid point and all the atoms of the polymer matrix that are subject to elastic fluctuations. These data are used to identify minimum energetic sites and determine transition probabilities from site to site together with the residence times in each site.

In the second step a Monte Carlo simulation of gas diffusion by a 'hopping' mechanism has been performed based on the energy as well as connectivity of sites and the transition jump probabilities. In this study, the smearing factor has been computed using the self-consistent field (SCF) procedure. The Mean Square Displacement (MSD) of all subsets of atoms in the amorphous cell is obtained as a function of time from a short NVT dynamics (30 ps with 1 fs time step at 300°K).

3. Results and Discussion

The protocol that we have used in this study for generating the models of the PEEKs membranes combined with the intermediary control of free volume distribution in the matrix have increased the reproducibility model cells construction. This has been validated by the TST simulations which show reduced differences between predicted S and D values of the same gas in different model cells of the same polymer. In the following we report results of the performed calculations.

3.1 Construction of realistic amorphous models

It has been clearly shown in the literature[12, 15, 21, 22, 24, 30] that the transport properties of small gases through glassy polymer membranes are strongly controlled by

the free volume and its distribution. For this reason the amorphous cells models of the PEEKs have been generated using a single polymer chain only, in order to minimize chain end effects, which would lead to increased density of chain ends and consequently would imply an increased free volume. In this study we have further “optimised” the idea of solvent inclusion in generating the amorphous cells. Before starting the packing of the polymer chain in the cell we insert 200 methanol molecules as well as three time 200 Argon atoms. This allows a much more “homogeneous” packed chain configuration as well as a more uniform free volume distribution within the matrix. The reason why the solvent has been introduced is that it can be removed in several stages while compressing the cell in order to increase the density. The “solvent insertion” step reduces considerably the probability of finding catenated phenylene rings or a sparring of side groups or backbone chains through ring sub-structures.

Polymer	Amorphous cells	Density (g/cm ³)	Access. Volume (Å ³)/cell	Surf/ Access. Vol. Ratio	D(O ₂) (cm ³ /s)* 10 ⁻⁶	S(O ₂) (cm ³ (STP) /cm ³ ·Pa)* 10 ⁻⁵
PEEKWC	Cell_1	1.173	1332.31	1.63	1.81	2.11
	Cell_2	1.179	1725.15	1.38	3.03	2.01
	Cell_3	1.181	1684.58	1.59	3.85	1.95
DMPEEK	Cell_1	1.394	791.81	1.47	1.60	1.89
	Cell_2	1.041	4960.52	0.89	1.13	1.75
	Cell_3	1.081	2668.84	1.38	6.88	2.03
TMPEEK	Cell_1	1.131	1332.31	1.63	1.81	2.11
	Cell_2	1.094	1725.15	1.38	3.03	2.01
	Cell_3	1.095	1684.58	1.59	3.85	1.95
DIDMPEEK	Cell_1	1.063	1652.71	1.57	2.05	1.94
	Cell_2	1.042	2451.20	1.54	4.28	1.98
	Cell_3	1.041	2716.77	1.32	3.27	2.01

Table 2: Free volume analysis of generated amorphous cells using a 1.7Angstrom probe.

After each step of solvent removal, several cycles of an initial energy minimization followed by a brief NVT run at 303 K and then a final energy minimization has been performed. After the removal of the last set of argon atoms and the carrying out of the NVT dynamics, followed by the energy minimisation, the density of the generated cells corresponded to nearly 90% of the experimental value.

In Table 2 we report the calculated data for 12 PEEKs cells using a probe with a radius

of 1.7 Angstrom (that correspond to the kinetic diameter of oxygen molecule). The accessible surface area (ASA) and accessible volume (AV) were calculated with the Free Volume utility of the Visualizer module of the Cerius2 4.2 software package[58] using the “Accessible” mode together with the “Fine” grid spacing specifications. A spherical probe atom with a defined radius R is rolled inside the amorphous cell polymer packing generating a diffusion-accessible surface. The accessible volume for a probe of radius R is defined as volume in the polymer matrix traced out by the probe’s centre for all the regions in which the probe can fit. The occupiable volume is just the accessible volume for a penetrant with radius $R = 0 \text{ \AA}$. By varying the probe radius it is possible to generate a series of ASA and AV values for each polymer packing and using an in-house MATLAB program to tabulate and plot the variation of ASA to AV ratio as well as its gradient. The calculations have been repeated systematically by varying the probe radius in the interval between 1.2 and 2.1 \AA , with a 0.1 \AA as step. The analysis of the obtained data allowed us to establish a correlation between the variation of the ratio between accessible Surface and accessible Volume, as well as its gradient, with the pore radius and the goodness of the cells. We report in Figure 2 the variation of these quantities for the 3 generated models of DMPEEK. On the basis of their variations we have excluded the cell_2 of this polymer from our further simulation. We have thus generated a new cell in order to have 3 final membrane structures for each of polymers.

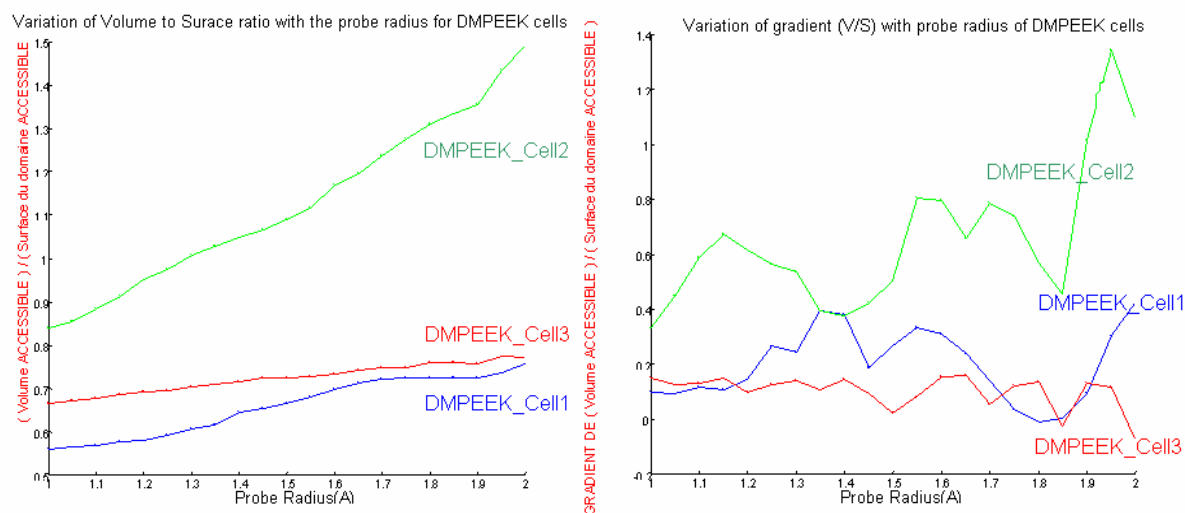


Figure2: Variation of Volume to Surface ratio and its gradient with probe radius.

1
2
3
4
5 The successive step, besides the check on the quality of boxes at an intermediate stage,
6 has been the reaching of the experimental density by increasing the pressure with
7 several cycles of NPT-MD (constant particle number, temperature and pressure) runs at
8 pressures of thousands of bars. Moreover, simulated annealing runs with temperatures
9 up to 1000 K and NVT dynamics at 303 K have been used to further relax the polymeric
10 structures. Equilibration and density adjustment of the polymer system have been
11 achieved through a final 300 picoseconds (ps) MD run.

12 It is worth to say that small deviations in obtaining the experimental density may
13 happen for glassy stiff-chain polymer materials[10, 15, 40] particularly if the models are
14 rather large. The deviations may reflect minor errors of the parameterization of the
15 respective polymers in the chosen force field, which influence the equilibration of the
16 models. In Table 3 we report the Free volume analysis results for the equilibrated
17 membrane model membrane packings using a probe with 1.7 Angstroms.

28 29 **3.2 TST prediction of gas transport properties**

30
31
32 The equilibrated amorphous cells are used in the TST calculations for estimating the
33 solubilities and diffusion coefficients for O₂, N₂ and CO₂ molecules for each cell. It is to
34 notice that the TST calculations using the gsdiff/gsnet software code[59, 60] assume
35 that the penetrant molecules are spherical united atoms characterised by effective
36 Lennard–Jones parameters (σ, ϵ) expressed in (Angstroms, kcal/mol). In all the
37 calculations we have used the default values of these parameters O₂(3.460, 0.2344),
38 N₂(3.698, 0.1889) and CO₂(4.000, 0.4500). In Tables 4 and 5 are reported respectively
39 the results of TST simulations and experimental measurements for O₂, N₂ and CO₂
40 molecules for the 12 equilibrated amorphous cells of the selected PEEKs. The
41 interaction energy between each gas molecule and the polymer matrix is calculated on
42 all node positions of the fine grid layered over the amorphous polymer packing cells. It
43 is to notice that only the Van der Waals (Lennard-Jones potentials) interactions are
44 considered. Furthermore it is assumed that the polymer packing does not have to
45 undergo structural relaxation (e.g. resulting from torsion transitions) to accommodate an
46 inserted particle. Therefore, this simulation technique is restricted to small molecules.
47 From Table 4 it appears clear that the simulated values are more self-consistent showing
48 less scatter than in recently reported papers dealing with modeling of alkylated PEEK
49
50
51
52
53
54
55
56
57
58
59
60

1
2
3
4
5 membranes[14, 39, 40] confirming in this way the new simulation protocol for
6 generating realistic amorphous cells models of these membranes. An inspection of
7 reported values in Table 4 and Table 5 indicates that a relatively good agreement is
8 obtained for O₂ and N₂ molecules and important deviations between simulated and
9 experimental values are observed for CO₂ for diffusion coefficient as well as the
10 solubility. It is important to notice that if one compares only the permeabilities, due to
11 an error compensation for the CO₂, would come to the conclusion that its transport
12 properties through alkylated PEEK membranes are better represented than those of O₂
13 and N₂. In order to analyse the discrepancies between experimental and simulated
14 results we report in Table 6 the ratio of simulated to experimental values of D and S at
15 300K for N₂, O₂ and CO₂ molecules for the 12 generated cells together with a
16 comparison of simulated to experimental ideal separation factors α_{O_2,N_2} and α_{N_2,CO_2} .
17 The reported experimental to simulated D ratio values indicate that the TST simulated
18 results for N₂ and O₂ are overestimated by a factor varying between 1.1 to 9.1 with
19 respective (mean, standard deviation) for O₂(4.1, 2.3) and N₂ (4.2, 2.7). On the contrary
20 the TST simulated results for CO₂ are underestimated
21 by a factor varying between 8.7 to 67.2. The tabulated experimental to simulated S ratio
22 values show the TST simulated results for N₂ and O₂ overestimated by a factor varying
23 between 2.3 to 4.7 (mean, standard deviation) respectively for O₂(3.97, 0.52) and N₂
24 (3.08, 0.54). The TST simulated results for CO₂ are also overestimated by a factor
25 varying between 4.6 to 17.3 with (mean, standard deviation) of (10.5, 4.7).
26
27
28
29
30
31
32
33
34
35
36
37
38
39
40
41
42
43
44
45
46
47
48
49
50
51
52
53
54
55
56
57
58
59
60

Model		Free Volume with Probe radius of 1.7 Å							
Polymer	Density (g/cm ³)	Available Volume (Å ³)	Occupiable Volume (Å ³)	Accessible Volume (Å ³)	Surface Area	FFV	Fractional Occupiable Vol (%)	Fractional Accessible (%)	S(Acc) / V(Acc)
PEEKWC	1.25	18146.2	194.6	93.5	146.4	0.083	0.328	0.158	1.565
	1.25	18169.9	236.9	101.0	135.4	0.084	0.399	0.179	1.341
	1.25	18142.4	192.4	111.9	160.3	0.083	0.324	0.189	1.433
DMPEEK	1.247	18659.9	267.5	145.0	203.9	0.072	0.425	0.231	1.406
	1.247	18583.4	240.7	79.7	126.5	0.070	0.383	0.127	1.587
	1.247	18644.9	284.7	136.6	215.9	0.071	0.453	0.217	1.581
TMPEEK	1.195	21688.1	328.3	105.3	152.3	0.094	0.475	0.152	1.447
	1.195	21681.7	285.6	127.7	197.9	0.094	0.413	0.185	1.550
	1.195	21696.1	281.0	89.4	132.1	0.094	0.407	0.129	1.478
DIDMPEEK	1.14	25805.5	501.6	121.0	181.3	0.107	0.629	0.152	1.498
	1.14	25856.0	525.9	214.8	319.8	0.108	0.659	0.269	1.489
	1.14	25837.6	471.6	201.8	307.8	0.107	0.591	0.253	1.525

Table3: Free volume analysis results for equilibrated cells using a 1.7Angstrom probe.

Model		TST								
Polymer	Density (g/cm ³)	O ₂			N ₂			CO ₂		
		D (cm ² /s)* 10 ⁻⁸	S (cm ³ (STP)/ cm ³ ·Pa)*10 ⁻⁵	Permeability (Barrer)	D (cm ² /s)* 10 ⁻⁸	S (cm ³ (STP)/ cm ³ ·Pa)* 10 ⁻⁵	Permeability (Barrer)	D (cm ² /s)* 10 ⁻⁸	S (cm ³ (STP)/ cm ³ ·Pa)* 10 ⁻⁵	Permeability (Barrer)
PEEKWC	1.25	4.7	1.47	9.25	1.1	0.87	1.33	0.017	48.20	1.10
	1.25	4.0	1.45	7.63	0.8	0.86	0.97	0.016	39.80	0.83
	1.25	2.8	1.23	4.51	0.7	0.70	0.63	0.011	30.80	0.46
DMPEEK	1.247	8.5	1.50	16.98	1.3	0.89	1.56	0.037	39.00	1.90
	1.247	12.7	1.23	20.89	2.1	0.74	2.02	0.052	31.80	2.19
	1.247	7.6	1.60	16.29	1.1	0.97	1.43	0.024	44.55	1.44
TMPEEK	1.195	22.2	1.61	47.74	3.6	0.91	4.29	0.071	36.10	3.42
	1.195	23.2	1.26	39.00	3.6	0.69	3.33	0.122	22.80	3.71
	1.195	26.4	1.45	50.97	4.6	0.77	4.75	0.140	26.51	4.94
DIDMPEEK	1.14	15.7	1.45	30.40	4.0	0.84	4.51	0.1	27.20	3.41
	1.14	26.8	1.52	50.79	6.9	0.81	7.43	0.209	23.20	6.52
	1.14	30.4	1.26	51.11	7.8	0.74	7.67	0.223	24.00	7.13

Table4: TST predicted S and D values of O₂, N₂ and CO₂ in selected PEEKs.

Model		Experimental data								
Polymer	Density (g/cm ³)	O ₂			N ₂			CO ₂		
		Diffusion (cm ² /s)* 10 ⁻⁸	Solubility (cm ³ (STP)/ cm ³ ·Pa)* 10 ⁻⁵	Permeability (Barrer)	Diffusion (cm ² /s)* 10 ⁻⁸	Solubility (cm ³ (STP)/ cm ³ ·Pa)* 10 ⁻⁵	Permeability (Barrer)	Diffusion (cm ² /s)* 10 ⁻⁸	Solubility (cm ³ (STP)/ cm ³ ·Pa)* 10 ⁻⁵	Permeability (Barrer)
PEEKWC	1.25	2.15	0.343	0.95	0.618	0.243	0.193	0.746	2.835	2.73
DMPEEK	1.247	1.96	0.344	0.87	0.295	0.251	0.095	0.639	3.151	2.6
TMPEEK	1.195	3.31	0.363	1.55	0.516	0.281	0.187	1.22	3.467	5.44
DIDMPEEK	1.14	9.12	0.413	4.85	2.25	0.322	0.936	3.83	5.129	19.3

Table 5: Experimental values of transport properties of O₂, N₂ and CO₂ in selected PEEKs.

The large deviations for CO₂ might be explained by the well known experimental fact of plasticisation of glassy membranes due to specific interactions of CO₂ with the polymer matrix leading to membrane structural relaxations. This behavior “violates” the assumption of the TST in which the dynamics of the dissolved molecules is coupled only to the elastic thermal motion of the dense polymer. The results for CO₂ show clearly the necessity to develop improved TST-methods which permit the matrix to be locally flexible in order to accommodate larger penetrant molecules that are described in all-atom with partial charges representation. A better agreement between simulated and experimental D and S for N₂ and O₂ could be easily obtained by re-parametrisation of Lennard-Jones parameters of the both gas molecules but this was not the objective of this study.

Polymer	Model .car/ .arc	D _{(Exp)/D_(Calc)}			S _{(Exp)/S_(Calc)}			Exp.		Calc.	
		O ₂	N ₂	CO ₂	O ₂	N ₂	CO ₂	P _{(O₂)/}	P _{(CO₂)/}	P _{(O₂)/}	P _{(CO₂)/}
								P _(N₂)	P _(N₂)	P _(N₂)	P _(N₂)
PEEKWC	cell_1	0.46	0.54	43.6	0.23	0.27	0.058	4.92	2.87	6.97	0.12
	cell_2	0.54	0.73	47.8	0.23	0.28	0.071	4.92	2.87	7.84	0.11
	cell_3	0.78	0.90	67.2	0.27	0.34	0.058	4.92	2.87	7.12	0.10
DMPEEK	cell_1	0.23	0.23	17.5	0.22	0.28	0.079	9.16	3.98	10.91	0.11
	cell_2	0.15	0.14	12.4	0.27	0.33	0.097	9.16	3.98	10.34	0.10
	cell_3	0.26	0.27	26.4	0.21	0.25	0.069	9.16	3.98	11.39	0.09
TMPEEK	cell_1	0.15	0.15	17.2	0.22	0.30	0.094	8.29	3.51	11.12	0.07
	cell_2	0.14	0.14	10.0	0.28	0.40	0.149	8.29	3.51	11.70	0.10
	cell_3	0.13	0.11	8.7	0.25	0.36	0.128	8.29	3.51	10.74	0.10
DIDMPEEK	cell_1	0.58	0.56	40.7	0.28	0.37	0.185	5.18	3.98	6.75	0.11
	cell_2	0.34	0.33	18.3	0.29	0.39	0.215	5.18	3.98	6.84	0.13
	cell_3	0.30	0.29	17.2	0.32	0.43	0.210	5.18	3.98	6.66	0.14

Table 6: Comparison of the ratio of experimental to simulated D, S for O₂, N₂ and CO₂ together with separation factors α_{O_2,N_2} and α_{N_2,CO_2} in selected PEEKs

In Table 7 the comparison of predicted to experimental diffusion and solubility selectivities reinforces the conclusions obtained from the analysis of Table 6. The predicted diffusion selectivity $[\alpha(D)_{O_2,N_2}]$ nicely reproduces the experimentally observed trend for O₂ and N₂ diffusion while the predicted $[\alpha(D)_{CO_2,N_2}]$ it is more than

one order of magnitude off the experimental values. The predicted trend for solubility selectivity for O₂ and N₂ [$\alpha(S)_{O_2,N_2}$] is in perfect agreement with the experimental observation with a slightly higher estimation of relative O₂ solubility. The predicted solubility selectivity for CO₂ and N₂ [$\alpha(S)_{CO_2,N_2}$] is more than 3 times higher than the experimental one.

Polymer	Model .car/ .arc	D _(selectivity)				S _(selectivity)			
		Exp (O ₂ /N ₂)	Sim (O ₂ /N ₂)	Exp (CO ₂ /N ₂)	Sim (CO ₂ /N ₂)	Exp (O ₂ /N ₂)	Sim (O ₂ /N ₂)	Exp (CO ₂ /N ₂)	Sim (CO ₂ /N ₂)
PEEKWC	cell_1	4.05	4.3	1.70	0.020	1.28	1.69	15.92	55.40
	cell_2	4.05	5.0	1.70	0.019	1.28	1.69	15.92	46.28
	cell_3	4.05	4.0	1.70	0.016	1.28	1.76	15.92	44.00
DMPEEK	cell_1	6.64	6.5	2.17	0.042	1.37	1.69	12.56	43.82
	cell_2	6.64	6.0	2.17	0.070	1.37	1.66	12.56	42.97
	cell_3	6.64	6.9	2.17	0.025	1.37	1.65	12.56	45.93
TMPEEK	cell_1	6.41	6.2	2.36	0.078	1.29	1.77	12.32	39.67
	cell_2	6.41	6.4	2.36	0.177	1.29	1.83	12.32	33.04
	cell_3	6.41	5.7	2.36	0.182	1.29	1.88	12.32	34.43
DIDMPEEK	cell_1	3.48	3.9	1.21	0.119	1.41	1.73	11.68	32.38
	cell_2	3.48	3.9	1.21	0.258	1.41	1.88	11.68	28.64
	cell_3	3.48	3.9	1.21	0.301	1.41	1.70	11.68	32.43

Table 7: Comparison of predicted to experimental Diffusion selectivities and Solubility selectivities for (O₂, N₂) and (N₂, CO₂) in selected PEEKs

4. Conclusions

A new protocol for packing glassy polymer with intermediate control of free volume distribution has been applied for four alkylated PEEKs, namely dimethyl PEEK-WC (DMPEEK), tetramethyl PEEK-WC (TMPEEK) and di-isopropyl dimethyl PEEK WC (DIDMPEEK). The TST approach of Gusev-Suter methodology was used to calculate diffusion and solubility coefficients for N₂, O₂, and CO₂ gas molecules in the generated membrane models. The comparison of modelled values of modified PEEK-WC with the experimental ones indicates that the new approach of packing produces amorphous cells

1
2
3
4
5
6
7
8
9
10
11
12
13
14
15
16
17
18
19
20
21
22
23
24
25
26
27
28
29
30
31
32
33
34
35
36
37
38
39
40
41
42
43
44
45
46
47
48
49
50
51
52
53
54
55
56
57
58
59
60

that show less scatter in predicted S and D values with respect to recent published papers dealing with these membranes[14, 39, 40]. A better agreement between simulated and experimental permeabilities could be obtained for improving prediction of absolute gas transport properties in glassy polymer membranes by re-parametrisation of Lennard-Jones parameters of the penetrant gas molecules.

Acknowledgement:

The work was in part supported by the European Commission 6th Framework Program Project MULTIMATDESIGN "Computer aided molecular design of multifunctional materials with controlled permeability properties "Contract Number: NMP3-CT-2005-013644".

5. References

- [1] P. V. K. Pant and R. H. Boyd, (1992) Simulation of diffusion of small penetrants in polymers in *Macromolecules*, 114, 494.
- [2] P. V. K. Pant and R. H. Boyd, (1993) Molecular-dynamics simulation of diffusion of small penetrants in polymers in *Macromolecules*, 26, 679.
- [3] F. Müller-Plathe, (1994) Permeation of polymers - a computational approach in *Acta Polymerica*, 45, 259.
- [4] A. A. Gusev, F. Muller-Plathe, W. F. Van Gunsteren, and U. W. Suter, (1994) Dynamics of small molecules in bulk polymers in *Advances in Polymer Science*, 116, 207.
- [5] P. V. K. Pant and D. N. Theodorou, (1994) A strategy for atomistic Monte Carlo simulation of polydisperse polymer systems in *Polymer Preprints (American Chemical Society, Division of Polymer Chemistry)*, 35, 165.
- [6] D. Hofmann, J. Ulbricht, D. Fritsch, and D. Paul, (1996) Molecular modelling simulation of gas transport in amorphous polyimide and poly(amide imide) membrane materials in *Polymer*, 37, 4773.
- [7] H. Takeuchi and K. Okazaki, (1996) Dynamics of small molecules in a dense polymer matrix: molecular dynamics studies in *Molecular Simulation*, 16, 59.

- 1
2
3
4
5
6
7 [8] J. R. Fried and D. K. Goyal, (1998) Molecular simulation of gas transport in poly[1-
8 (trimethylsilyl)-1-propyne] in *Journal of Polymer Science, Part B: Polymer Physics*, 36,
9 519.
- 10
11 [9] R. K. Bharadwaj and R. H. Boyd, (1999) Small molecule penetrant diffusion in
12 aromatic polyesters: a molecular dynamics simulation study in *Polymer*, 40, 4229.
- 13
14 [10] D. Hofmann, L. Fritz, J. Ulbrich, C. Schepers, and M. Bohning, (2000) Detailed-
15 atomistic molecular modeling of small molecule diffusion and solution processes in
16 polymeric membrane materials in *Macromolecular Theory and Simulations*, 9, 293.
- 17
18 [11] M. Lopez-Gonzalez, E. Saiz, J. Guzman, and E. Riande, (2001) Experimental and
19 simulation studies on the transport of gaseous diatomic molecules in polycarbonate
20 membranes in *J. Chem. Phys.*, 115, 6728.
- 21
22 [12] F. Muller-Plathe, (2001) Molecular simulation of polymers: from concepts to industrial
23 applications in *DECHEMA Monographien*, 137, 163.
- 24
25 [13] R. Shanks and D. Pavel, (2002) Simulation of diffusion of O₂ and CO₂ in amorphous
26 poly(ethylene terephthalate) and related alkylene and isomeric polyesters in *Molecular*
27 *Simulation*, 28, 939.
- 28
29 [14] E. Tocci, E. Bellacchio, N. Russo, and E. Drioli, (2002) Diffusion of gases in PEEKs
30 membranes: molecular dynamics simulations in *Journal of Membrane Science*, 206,
31 389.
- 32
33 [15] M. Heuchel, D. Hofmann, and P. Pullumbi, (2004) Molecular Modeling of Small
34 Molecule Permeation in Polyimides and its Correlation to Free Volume Distributions in
35 *Macromolecules*, 37(1), 201.
- 36
37 [16] N. C. Karayiannis, V. G. Mavrantzas, and D. N. Theodorou, (2004) Detailed atomistic
38 simulation of the segmental dynamics and barrier properties of amorphous
39 poly(ethylene terephthalate) and poly(ethylene isophthalate) in *Macromolecules*, 37,
40 2978.
- 41
42 [17] S. Neyertz and D. Brown, (2004) Influence of system size in molecular dynamics
43 simulations of gas permeation in glassy polymers in *Macromolecules*, 37, 10109.
- 44
45 [18] V. E. Raptis, I. G. Economou, D. N. Theodorou, J. Petrou, and J. H. Petropoulos, (2004)
46 Molecular dynamics simulation of structure and thermodynamic properties of
47 poly(dimethylsilamethylene) and hydrocarbon solubility therein: Toward the
48 development of novel membrane materials for hydrocarbon separation in
49 *Macromolecules*, 37, 1102.
- 50
51 [19] D. Hofmann, M. Entrialgo-Castano, A. Lerbret, M. Heuchel, and Y. Yampolskii, (2003)
52 Molecular modeling investigation of free volume distributions in stiff chain polymers
53 with conventional and ultrahigh free volume: Comparison between molecular modeling
54 and positron lifetime studies in *Macromolecules*, 36, 8528.
- 55
56
57
58
59
60

- 1
2
3
4
5
6
7 [20] D. Hofmann, M. Heuchel, Y. Yampolskii, V. Khotimskii, and V. Shantarovich, (2002)
8 Free Volume Distributions in Ultrahigh and Lower Free Volume Polymers: Comparison
9 between Molecular Modeling and PALS Studies in *Macromolecules*, 35, 2129.
10
11 [21] B. D. Freeman, (1999) Basis of permeability/selectivity tradeoff relations in polymeric
12 gas separation membrane in *American chemical society*, 32, 375.
13
14 [22] S. A. Stern and W. J. Koros, (2000) Separation of gas mixtures with polymer
15 membranes a brief overview in *Chimie Nouvelle*, 18, 3201.
16
17 [23] L. M. Robeson, W. F. Burgoyne, M. Langsam, A. C. Savoca, and C. F. Tien, (1994)
18 High performance polymers for membrane separation in *Polymer*, 35, 4970.
19
20 [24] L. M. Robeson, (2003) Structure/property studies on polymeric materials in *Abstracts*
21 of Papers, 225th ACS National Meeting, New Orleans, LA, United States, March 23-
22 27, 2003, POLY.
23
24 [25] L. M. Robeson, W. F. Burgoyne, M. Langsam, A. C. Savoca, and C. F. Tien, (1994)
25 High performance polymers for membrane separation in *Polymer*, 35, 4970.
26
27 [26] S. A. Stern, (1994) Polymers for gas separations : the next decade in *Journal of*
28 *membrane science*, 94, 1.
29
30 [27] C. M. Zimmerman, A. Singh, and W. J. Koros, (1997) Tailoring mixed matrix
31 composite membranes for gas separations in *Journal of Membrane Science*, 137, 145.
32
33 [28] W. J. Koros and G. K. Fleming, (1993) Membrane-based gas separation in *Journal of*
34 *Membrane Science*, 83, 1.
35
36 [29] L. M. Robeson, (1991) Correlation of separation factor versus permeability for
37 polymeric membranes in Elsevier Science Publishers, 165.
38
39 [30] W. J. Koros, M. R. Coleman, and D. R. B. Walker, (1992) Controlled permeability
40 polymer membranes in *Annual Revue Materials*, 22, 47.
41
42 [31] I. C. Roman, R. W. Ubersax, and G. K. Fleming, (2001) New directions in membranes
43 for gas separation in *Chimica e l'Industria (Milan, Italy)*, 83, e1/1.
44
45 [32] D. R. Paul and M. R. Pixton, (1997) Polyarylate gas separation membranes in
46 *Macromolecules Symp.*, 118, 401.
47
48 [33] H. C. Zhang, T. L. Chen, and Y. G. Yuan, (1987) Synthesis of new type polyether ether
49 ketone with phtalein lateral group in Chinese Patent,
50
51 [34] K. Liu, H. C. Zhang, T. L. Chen, and Y. G. Yuan, (1986) Single-step process for
52 synthesizing polyarylethersulfones with peptide side chain in Chinese Patent,
53
54 [35] F. Lufrano, E. Drioli, G. Golemme, and L. Di Giorgio, (1996) Transport parameters of
55 carbon dioxide in PEEK membr. in *Journal of Membrane Science*, 113, 121.
56
57 [36] M. G. Buonomenna, A. Figoli, J. C. Jansen, and E. Drioli, (2004) Preparation of
58 asymmetric PEEKWC flat membranes with different microstructures by wet phase
59 inversion in *Journal of Applied Polymer Science*, 92, 576.
60

- 1
2
3
4
5
6
7 [37] F. Tasselli, J. C. Jansen, and E. Drioli, (2004) PEEKWC ultrafiltration hollow-fiber
8 membranes: Preparation, morphology, and transport properties in *Journal of Applied*
9 *Polymer Science*, 91, 841.
- 10
11 [38] J. C. Jansen, M. Macchione, and E. Drioli, (2005) High flux asymmetric gas separation
12 membranes of modified poly(ether ether ketone) prepared by the dry phase inversion
13 technique in *Journal of Membrane Science*, 255, 167.
- 14
15 [39] E. Tocci, M. P. Perrone, N. Russo, and E. Drioli, (2005) Molecular simulations of gas
16 transport properties of alkylated PEEK membr. in *J. Mol. Graph. and Model.*, in press.
- 17
18 [40] E. Tocci, D. Hofmann, D. Paul, N. Russo, and E. Drioli, (2001) A molecular simulation
19 study on gas diffusion in a dense poly(ether-ether-ketone) membr. in *Polymer*, 42, 521.
- 20
21 [41] D. N. Theodorou and U. W. Suter, (1985) Detailed molecular structure of a vinyl
22 polymer glass in *Macromolecules*, 18, 1467.
- 23
24 [42] Z. Wang, T. Chen, and J. Xu, (2000) Gas Transport Properties of Novel Cardo Poly(aryl
25 ether ketone)s with Pendant Alkyl Groups in *Macromolecules*, 33, 5672.
- 26
27 [43] I. Accelrys, (2004) Accelrys, Inc. San Diego, CA, USA. [InsightII(400P+) software
28 package]
- 29
30 [44] D. Rigby, H. Sun, and B. E. Eichinger, (1997) Computer Simulations of Poly(ethylene
31 oxide): FF, PVT Diagram and Cyclization Behavior in *Polymer international*, 44, 311.
- 32
33 [45] J. Bicerano, *Prediction of polymer properties* 2nd ed., Dekker Marcel, New York, 1996.
- 34
35 [46] H. J. Meriovitch, (1983) Computer Simulation of Self-Avoiding Walks: Testing the
36 Scanning Method in *J. Chem. Phys.*, 79, 502.
- 37
38 [47] W. J. Koros and G. K. Fleming, (1993) Membrane-based gas separation in *Journal of*
39 *Membrane Science*, 83, 1.
- 40
41 [48] Sok, Berendsen, and Gunsteren, (1992) Molecular dynamics simulation of the transport
42 of small molecules across a polymer membr. in *Journal Chemistry Physical*, 96, 4699.
- 43
44 [49] S. A. Stern, (1994) Polymers for gas separations: the next decade in *Journal of*
45 *Membrane Science*, 94, 1.
- 46
47 [50] N. F. A. Van der Vegt, (2000) Temperature Dependence of Gas Transport in Polymer
48 Melts: Molecular Dynamics Simulations of CO₂ in Polyethylene in *Macromolecules*,
49 33, 3153.
- 50
51 [51] A. A. Gusev and U. W. Suter, (1993) Dynamics of small molecules in dense polymers
52 subject to thermal motion in *J. Chem. Phys.*, 99, 2228.
- 53
54 [52] Gusev, Arizzi, and Suter, (1993) Dynamics of light gases in rigid matrices of dense
55 polymers in *Journal Chemistry Physical*, 99, 2221.
- 56
57 [53] D. N. Theodorou and U. W. Suter, (1986) Atomistic modeling of mechanical properties
58 of polymeric glasses in *Macromolecules*, 19, 139.
- 59
60 [54] I. Accelrys, (2004) Accelrys, Inc. San Diego, CA, USA. [InsightII(400P+) software
package] *Polymer User Guide*. Polymerizer section.

- 1
2
3
4
5
6
7 [55] H. Sun and D. Rigby, (1997) Polysiloxanes: Ab Initio Force Field and Structural,
8 Conformational and Thermophysical Properties in *Spectrochimica Acta Part A*, 153,
9 1301.
10
11 [56] T. A. Andrea, W. C. Swope, and H. C. Andersen, (1983) The Role of Long Ranged
12 Forces in Determining the Structure and Properties of Liquid Water in *J. Chem. Phys.*,
13 79, 4576.
14
15 [57] H. J. C. Berendsen, J. P. M. Postma, W. F. Van Gunsteren, A. DiNola, and J. R. Haak,
16 (1984) Molecular dynamics with coupling to an external bath. in *J. Chem. Phys.*, 81,
17 3684.
18
19 [58] I. Accelrys, (2004) Accelrys, Inc. San Diego, CA, USA. [Cerius2 software package]
20
21 [59] I. Accelrys, (2000) Implemented as gsnet/gsdiff in InsightII(400P+) Accelrys, Inc.
22
23 [60] A. Tiller, (1993) Implemented as gsnet/gsdiff code in InsightII (400P+) molecular
24 modeling software package. Accelrys, Inc.
25
26
27
28
29
30
31
32
33
34
35
36
37
38
39
40
41
42
43
44
45
46
47
48
49
50
51
52
53
54
55
56
57
58
59
60